International Journal of Research Publication and Reviews

Journal homepage: www.ijrpr.com ISSN 2582-7421

Pore Pressure Studies in the Agbada Field in the Central Swamp Niger Delta, Nigeria

Okey U. Justus[1], Etim D. Uko[2], Onengiyeofori A. Davies[3] and Iyeneomi Tamunobereton-ari[4]

[1,2,3,4]*Department of Physics, Rivers State University, P. M. B. 5080, Port Harcourt, Nigeria*

A B S T R A C T

Pore pressure prediction ahead of drilling is a key requirement for safe and economic drilling of deep wells. Pore pressure, vertical effective stress, fracture gradient and overburden pressure gradient can be estimated from seismic velocities. However, there must be a good velocity to pore pressure transform, and the velocity used must be calibrated with well data, for accurate prediction to be obtained. Hence, this research was geared towards studying pore pressures as estimated from seismic data, calibrated with estimates made from well data in the Agbada Field in the Central Swamp area of the Niger Delta Petroleum basin. Well-log and seismic data were used for the work. The predicted shale pressures from the calibration well show a normal hydrostatic trend from the surface down to about 10, 800 ftss, where a transition to overpressure was noticed. The pressure transition zone for this area, as estimated from the calibration log, can be said to be between 10,887ftss to 11702ftss, where mild overpressures ranging from about 0.51psi to 0.52psi were observed. Furthermore, the top of geopressure is found at approximately 13,318ftss, from where hard overpressures ranging from 0.77 to 0.79psi occurred in the shale and much higher in the reservoirs. Two regional marker shale (maximum flooding surfaces) control the over-pressures in the area; 19.4ma MFS (11707ftss) and 20.7ma MFS (13934ftss). Additionally, the vertical effective stress estimated from the seismic data showed reversals around the well and beyond, where overpressures occurred. Also, the overburden pressure derived from seismic velocity showed that overburden pressure is affected by the density of sediments and the vertical effective stress. Furthermore, the seismic pore pressure profile showed the existence of mild to hard overpressures, with values as high as 0.82 psi/ft, within the vicinity of the calibration well. Finally, the estimated fracture gradient, defined relative to the pore pressure gradient, showed sudden jump in fracture gradient within the area of study, ranging in value from 0.68 psi/ft to 0.86 psi/ft. Seismic velocity and well-log data were in good agreement for the pore pressure profile in the area of study.

Keywords:Seismic and Well-Log Data, Pore Pressure Prediction, Pressure Gradient, Seismic Velocity, Niger Delta, Nigeria

1. Introduction

The conditions for the existence of abnormal pore pressures are observed in many sedimentary basins throughout the world (Osborne and Swarbrick, 1997; Gunter et al., 2004; Zahid and Uddin, 2005; Tingay et al., 2009; Udoh et al., 2022). Abnormal pore pressures are encountered worldwide, often resulting in drilling problems such as fluid kicks, well blowouts, borehole instability, stuck pipe and loss of circulation (Moucht and Mitchell, 1989; Sayers et al., 2002). In the drilling phase, an accurate pore-pressure prediction and the ability to update and revise predictions quickly can be vital in preventing pipe-stuck lost circulation of drilling fluids, resulting in costly lost rig time. Moreover, estimates of proper pore pressure and fracture pressure are also essential for an optimized casing program design and for avoiding well control problems, such as blowouts (Abdali et al., 2021). Pore pressure prediction is also significant in selection of drilling rigs. The knowledge of pore pressure is a key requirement for optimal well development decisions in overpressure areas, especially the Agbada field of the Niger Delta, where overpressures have caused some well drilling programs to be altered midway, with attendant cost implications and health, safety and environmental (HSE) risks.

Overpressures in sedimentary basins have many causes such as disequilibrium compaction (Neuzil, 1995; Swarbrick and Osborne, 2002; Traugott, 1997; Yardley and Swarbrick, 2000), tectonic compression, hydrocarbon generation, aquathermal expansion (Perry and Hower, 1972; Mouchet, Magara 1980 and Swarbrick and Osborne, 2002), mineral dehydration, mineral transformation, diapirism (Gilreath, 1968; Murray, 1961), vertical fluid movement, and hydrocarbon buoyancy (Osborne and Swarbrick, 1997; Nunn, 1996; Cathles, 2001; Chopra and Huffman, 2006; Schulz et al., 2009; Zhang,

* *Corresponding author.*Onengiyeofori A. Davies.
E-mail address: davies.onengiyeofori@ust.edu.ng

2011).Overpressures caused by disequilibrium compaction are related to undercompaction (anomalously high sediment porosities) and can be detectable in sonic log (Rubey and Hubbert, 1959; Johnson and Bredeson, 1971; Fertl, 1976; Dutta, 1987; Sayers et al., 2002; Tingay et al., 2009; Uko et al; 2013)

In the Niger Delta, well drilling and control operations have had a series of setbacks with several drillable prospects abandoned due to blowout problems (Ateboh & Raimi, 2018). As a consequence, reserve estimation is affected. The aim of the study is therefore to predict pore pressure profile ahead of drill bit, using seismic and oil and gas wells data in the Central Swamp Niger Delta, Nigeria. The result of this study can be used to eliminate pressure related well control problems such as gas kicks, blowouts, stuck pipe, loss circulation. The outcomes of this study can be used to design efficient mud weight programme for drilling for hydrocarbons in the region. Moreover, the results of this research can also be used to determine the appropriate selection of casing points, in order to reduce downtime and cost of drilling operations.

2. Geological Settings of the Area of Study

This research was carried out with data obtained from Agbada Field in the onshore Central swamp area of the Niger Delta, Nigeria. The Niger Delta is approximately 211,000 km^2 in surface area and developed south-westwards out of the Anambra Basin and the Benue Trough (Chilingar et al., 2002). It lies south of the West African shield and west of the Oban Massif and the Tertiary Cameroun Volcanic trend. The delta is located east of the Benin basin and its southern margin is marked by seafloor escarpments that lie over the oceanic crust. The map of the study area is shown in Fig. 1.

The structural development sets in during the Eocene/Lower Oligocene with the deposition of the Akata prodelta clays (about 6500m thick), which are overlain by deep-sea sandy fan deposits. The thickness of the Akata Shale reflects the post-rift structure of the oceanic crust. Agbada Formation (Fig. 2) is transitional between the upper Benin formation and the underlying Akata formation. It consists of a sequence of deltaic sands and shales. It is Eocene to Oligocene in age and consists of paralic siliciclastic that are more than 3500m thick (Corredor et al., 2005). It has micro fauna at the top while the base is characterized by a body of sandstone. The coarseness of the grains and poor sorting in this formation is indicative of its fluviatile origin. This formation serves as the main hydrocarbon reservoir due to hydrocarbon accumulation confined within it (Ejedawe, 1981)..

Benin Formation (Fig. 2) is the youngest unit in the Niger Delta. It is continental and consists of coastal plain sands, gravel with a few clay intercalations, consisting of late Eocene to recent deposits of alluvial and upper coastal plain deposits that are up to about 2000m thick (Ukpong & Anyanwu, 2018). It is a continental deposit of probable upper deltaic depositional environment (Reijers et al., 1996). It is Oligocene of age in the North on the subsurface and becomes younger progressively southward. Although this is the water bearing formation in the Niger Delta, very little hydrocarbon accumulation has been associated with this formation.

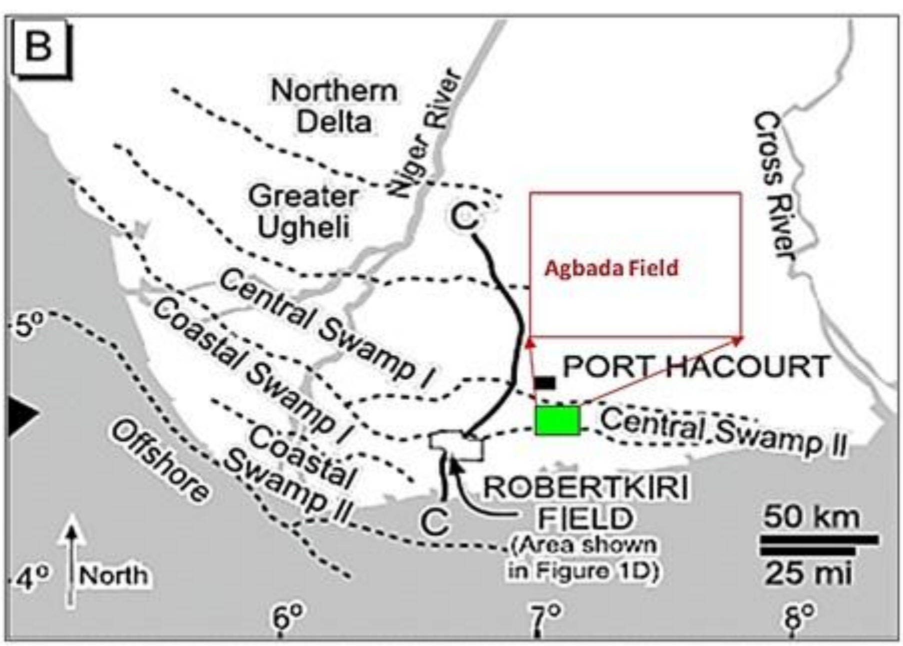

Fig. 1: Map of the Niger Delta showing the Study Area (Magbagbeola and Willis, 2007)

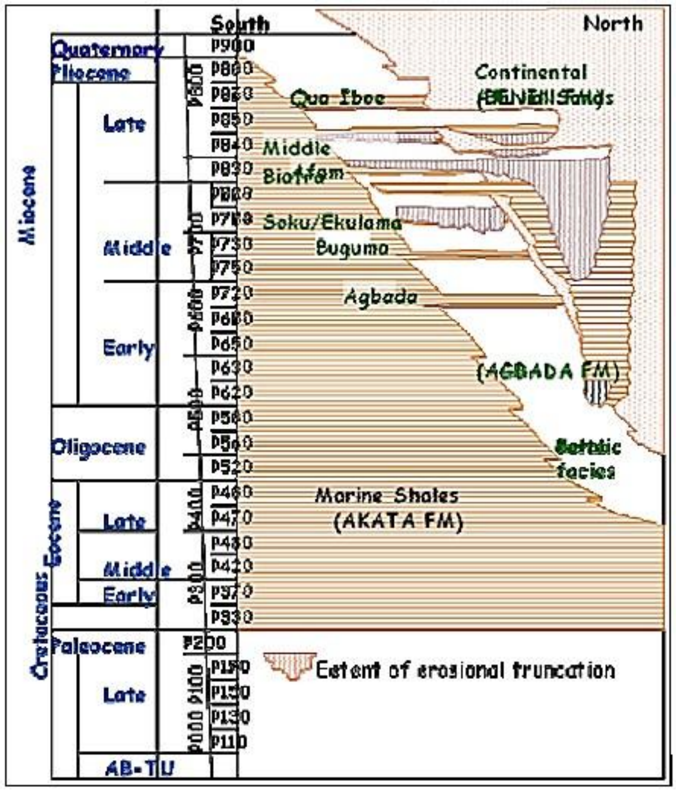

Fig. 2: Generalized Stratigraphy of the Central Swamp Area of the Niger Delta (Magbagbeola and Willis, 2007)

3. Methodology

3.1 Relevant Geo-Pressure Terms

Some pressure terms are necessary to be defined as used in this work. Pore pressure or formation pressure, P, is defined as the pressure acting on the fluids in the pore space of a formation. Hydrostatic pressure, P_h, is the pressure caused by the weight of a column of fluid, mainly water. Normal pressure (hydrostatic pressure or normal fluid pressure) is the pressure exerted by a static column of water of the same height as the overlying pore fluids and the same density as the pore water. It is usually expressed relative to fluid density (ρ_f), height of the fluid column (z) and the acceleration due to gravity (g) such that,

$$P_h = \rho_f g z \qquad (1)$$

The formation pressure gradient, expressed usually in pounds per square inch per foot (abbreviated by psi/ft), is the ratio of the formation pressure, P (in psi), to the depth, z (in feet). According to Shaker (2014), the hydrostatic pressure gradient, P_g (in psi/ft), is related to the fluid density, ρ_f (in g/cm^3) such that,

$$P_g = 0.433 \times \rho_f \qquad (2)$$

According to Sayers *et al.* (2006), overburden pressure, S (z), at any depth is the pressure which results from the combined weight of the rock matrix and the fluids in the pore space overlying the formation of interest, expressed as,

$$S(z) = g \int_0^z \rho_b(z) dz \qquad (3)$$

where ρ_b is the depth dependent bulk density. Evidently, the overburden pressure (also referred to as the geostatic or lithostatic pressure) is depth-dependent, increasing with depth.

The effective pressure or differential pressure or effective stress (σ) is the pressure, which is acting on the solid rock framework (Kumar et al., 2012). According to Terzaghi's principle (Terzaghi, 1943), effective pressure is defined as the difference between the overburden pressure, S, and the pore pressure, P.

$$\sigma = S - P \qquad (4)$$

All of the mechanisms listed above, in any combination, with the passage of geologic timework together to cause the changes in the physicochemical environment (Fertl, 1976);

3.2 Data/Software Required

The data used for this research included well log data from calibration well (gamma ray log, density log, sonic log, shale volume log and checkshot data), seismic interval velocity, regional hydrostatic gradient and overburden distribution.

Additionally, certain software was required to analyse the available dataset. These were all proprietary software of Shell Petroleum Development Company (SPDC) including RokDoc, 123DI and Vital.

3.3Estimation of Pore Pressure from Well Logs

To minimize error on the estimates made from the well logs due to washout and cycle skips, quality-control was carried out on the available well logs. As shown in the caliper log in Fig. 3, the control well logs have some washout issues. So, it was necessary to calibrate the sonic log with the well checkshot-derived velocity to correct for such errors.

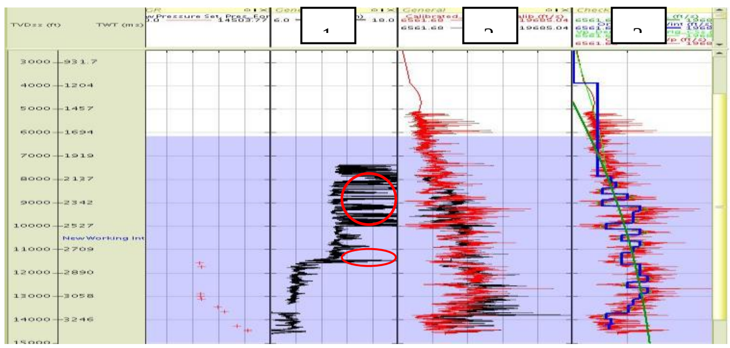

Fig. 3: Well logs from the calibration Well; Panel 1 is the calliper log with washout issues at depths circled

From the gamma ray log, shale intervals and sand tops and bases were then identified. Shale volume log was also generated from gamma ray log using the volume fract generator in Rokdoc. The generated shale volume log was then used alongside the calibrated sonic log as inputs to generate a shale trend velocity log. Additionally, from shale intervals that are not less than a threshold thickness and greater than threshold fraction shale content, , estimate of the normal compaction trend line (N.C.T) was made, with at least 90% or greater shale content and 10 feet minimum thickness considered. The NCT line corresponds to the expected increase in the density of shale formations as a function of depth, due solely to increasing hydrostatic pressure. It is produced by a best-fit linear regression of the log data at the valid shale depths. Since sonic log measures the interval transit time per foot of a formation, it became necessary to take the average of readings from the tops and bases of the shale intervals, bounding the over-pressured reservoirs, in order for the measured velocity to be representative of the entire shale interval sampled by the sonic wave

The overburden gradient S was then calculated from an integral of density according to equation 3. Additionally, the effective stress (ES) was estimated relative to the overburden stress and (PS) and the pore pressure (PP) according to equation 4. The shale pore pressure (PP_{Shale})was predicted from well logs relative to overburden pressure gradient (S), hydrostatic pressure gradient (H), observed shale sonic velocity (V_{Obs}), normal compacted shale sonic velocity (V_{Norm}) and Easton's exponient (N) using the Eaton's (1972) effective stress model for transforming velocity to pore pressure as defined by equation 5.

$$PP_{Shale} = S - (S - H) \times \left(\frac{V_{Obs}}{V_{Norm}}\right)^N \qquad (5)$$

The Eaton's exponent is a transformation exponent that is variable with age and basin. It describes the sensitivity of velocity to effective stress. For the Niger delta, the value is 3, which is the typical value of N for young clastic Tertiary basins like the Niger delta and the Gulf of Mexico (Okey et al.; 2021)

3.4 Prediction of Pore Pressure from Seismic Velocities

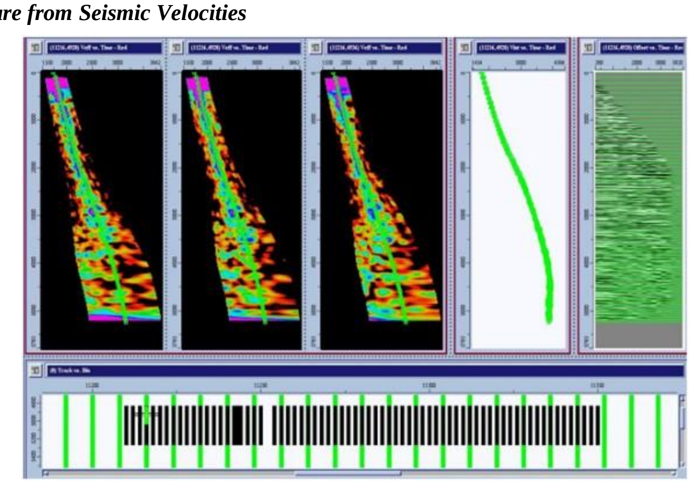

Fig. 4: Semblance Panel Velocity versus Time Display for Velocities Extraction from Seismic Volumes.

A fit-for-purpose velocity model was generated on a grid of 100m by 100m from the available root-mean-square (RMS) velocities for the area of interest, which ranges from track 11240 to track 11316 and bin 4972 to bin 5072 as shown in Fig. 4. The picked RMS velocities were then converted to interval velocities according to Dix (1955) equation given below,

$$V_{INT} = \sqrt{\frac{V_n^2 T_n - V_{n-1}^2 T_{n-1}}{T_n - T_{n-1}}} \qquad (5)$$

Where V_{INT} is interval velocity and $T_n$is the zero-offset arrival time corresponding to the n^{th} reflection. V_n is the root-mean-square velocity. The interval velocities were then calibrated with well data to yield the final earth velocity model, which was used for the pore pressure prediction.

One of the evidences that the seismic data has been correctly calibrated with the well data, is found in the crossplot of the fitted time depth pairs of checkshot and seismic data (Figs. 5aand 5b). The fitted time depth pair from seismic tracks that of the checkshot especially at depths where well controls exist. However,a significant deviation is clearly seen beyond those depths. Hence pore pressure prediction beyond the well total depth (TD) cannot be relied on. This is actually one limitation of pore pressure prediction from calibrated seismic velocities.

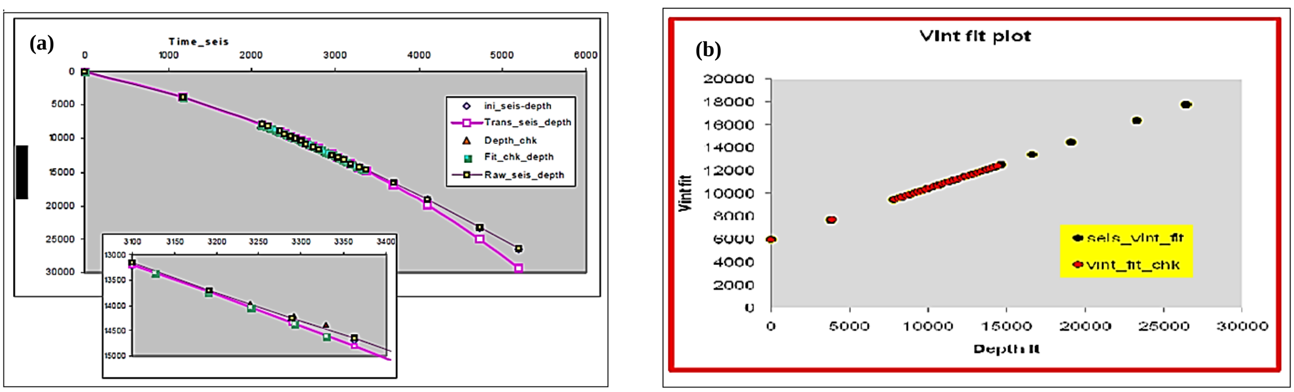

Fig. 5: (a) Semblance Panel Velocity versus Time Display for Velocities Extraction from Seismic Volumes. (b) Semblance Panel Velocity versus Time Display for Velocities Extraction from Seismic Volumes.

4. Results and Discussion

4.1 Estimation of Pore Pressure from Well Logs

The calibration well is a deep well, with total depth of 14,508 ftss originally drilled to test deep prospects in a rollover anticline structure, approximately between 12,000 and 15,500 ftss deep. The predicted shale pressures show a normal hydrostatic trend from the surface down to about 10, 800 ftss, where a transition to overpressure was noticed, as shown in Fig 6. The pressure increased in a step-wise manner down to about 11,702 ftss.

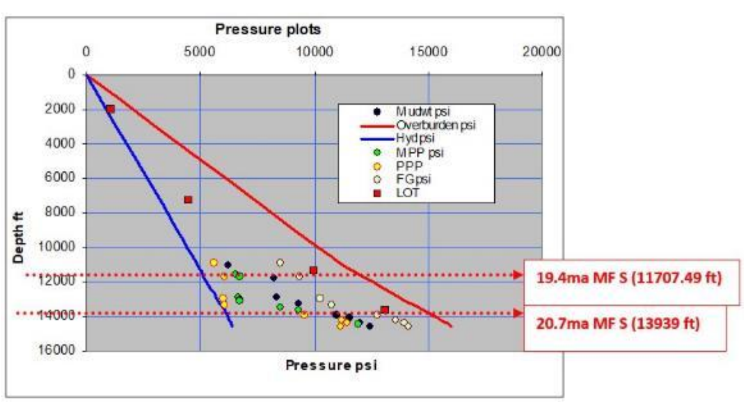

Fig. 6: Pore Pressure Profile for the Calibration Well, Predicted from valid Shale Intervals.

A drop in the predicted shale pressure of about 23psi was noticed between 11,703ftss and 13,318ftss, this is likely due to leakage across bounding fault induced by production from the hydrocarbon bearing P650 paralic sequence in the adjacent Okpodon field, 10 km north of the control well. This drop was also noticed in the reservoir, but of a much higher magnitude (800psi) and was responsible for the stuck pipe event at 13,038 ft which led to the sidetrack introduced in the drilling of the well. The pressure transition zone for this area can be said to be between 10,887ftss to 11702ftss, where mild overpressures ranging from about 0.51psi to 0.52psi were observed. The top of geopressure is found at approximately 13,318ftss, from where hard overpressures ranging from 0.77 to 0.79psi occurred in the shale and much higher in the reservoirs.

Two regional marker shale (maximum flooding surfaces) control the over-pressures in the area; 19.4ma MFS (11707ftss) and 20.7ma MFS (13934ftss). As observed in Fig. 6, there is a significant disparity between the reservoir pressures and the estimated shale pressures. This can be attributed to two factors; first, the well was drilled on a structural high, second buoyancy effects due to the presence of hydrocarbon in some units of the adjacent reservoirs. There seem to be a centroid depth around 14,208ftss, which might also be another factor. Usually above the centroid depth, the pore pressure in the sands exceeds that of the bounding shale.

4.2 Prediction of Pore Pressure from Seismic Velocities

Seismic interval velocity picked using the Umuechem 3D seismic data were available as a function of time on a grid of 200m by 200m spacing (Fig. 11). However, they were not suitable for pore pressure prediction because they were over-smoothed. A new fit-for-purpose velocity model was generated on a grid of 100m by 100m from the available rms velocities for the study area, which ranges from track 11240 to track 11316 and bin 4972 to bin 5072. A total of 494 velocity analysis points were picked around the calibration well and the prospect area (Fig.8). The rms velocities were then labeled and converted into interval velocities. The interval velocities were then calibrated with well data to yield the final earth velocity model, which was used for the pore pressure prediction.

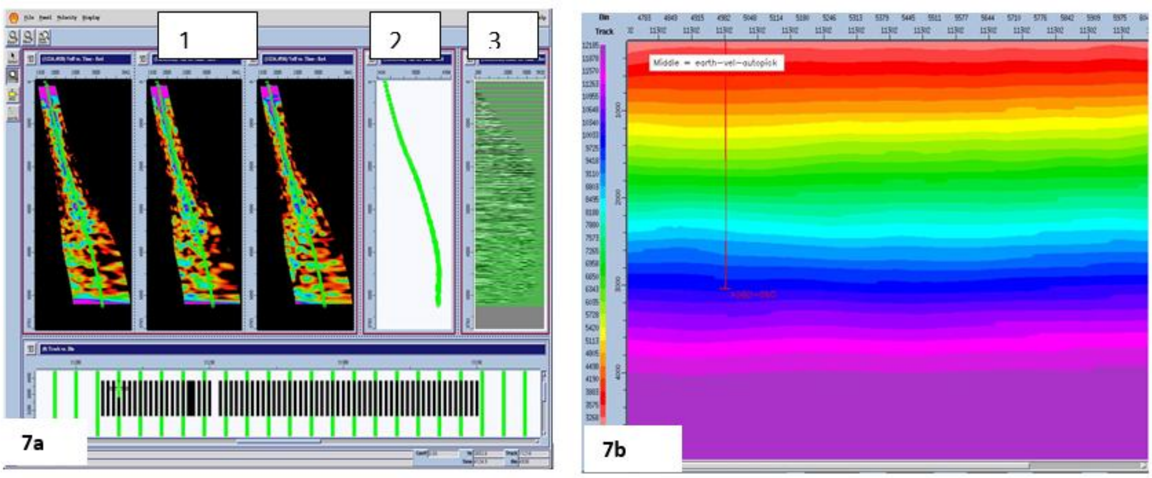

Fig. 7: (7a) Seismic velocity picking panel (7b) Initial Interval velocity model.

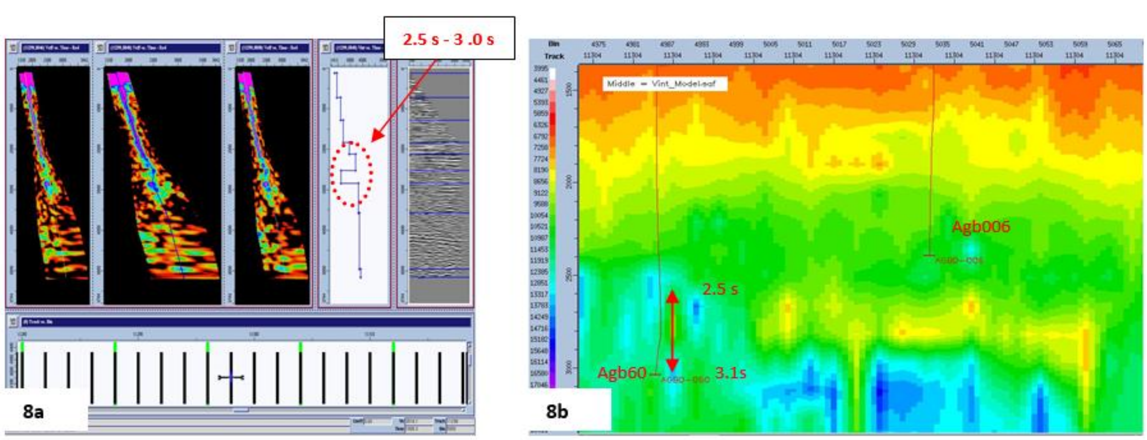

Fig. 8: (8a) Seismic velocity picking panel (8b) Final Interval velocity model.

Accurate calibration of the seismic velocity is a key requirement for predicting pore pressure from seismic velocity (Ifeanyi, 2015). The purpose of calibration is to slow down the seismic velocities in order to correct for anisotropy effects. This is necessary, to minimize time/depth mismatch in the final pore pressure model.

A correct calibration should have the time fit / depth curve from seismic, tracking the time fit/ depth curve from checkshots as shown in Fig. 9. The fit is very good down to about 14560 ftss, where well controls exist. Beyond that depth, there is an excursion of the seismic trend away from the well trend. However, the seismic velocity cannot be vouched for at depths greater than the maximum offset of the seismic survey. The maximum offset is 4.190 km, which is equivalent to 13747 ft (3.4seconds). The calibrated seismic velocity is the final earth model velocity that is used to calculate pore pressure.

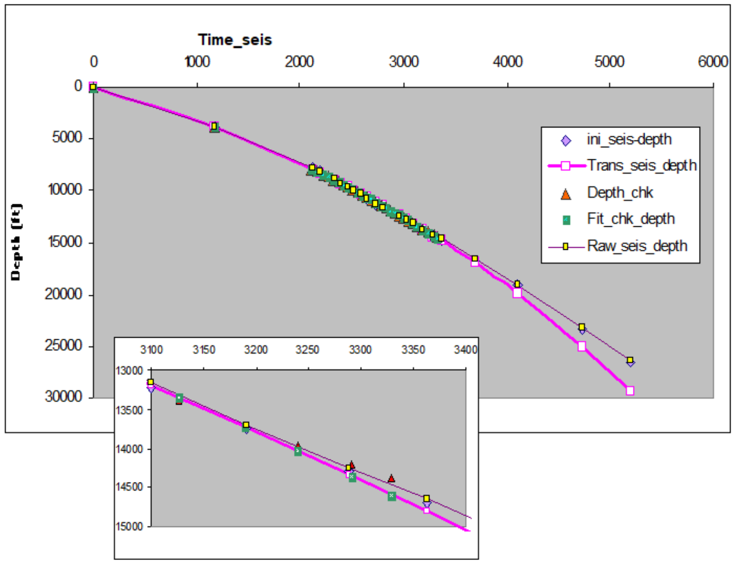

Fig. 9: The seismic time/depth pair tracks the checkshot time/depth pairs.

The effective stress model for transforming seismic velocities to pore pressure in shale is estimated as the difference between overburden pressure gradient and the vertical effective stress gradient as described by Terzaghi (1943). To estimate the VES from seismic velocity, the first step is to crossplot the well VES against the well sonic velocity as shown in Fig. 10. The regression equation is used with the seismic velocity to derive VES from seismic. The final VES model is shown in Fig. 11a. VES reversals can be seen around the well and beyond, where overpressures occurred. VES reversals actually correspond to an increase in porosity, and the occurrence of overpressures, especially if they are caused by disequilibrium compaction (Zhao et al., 2018).

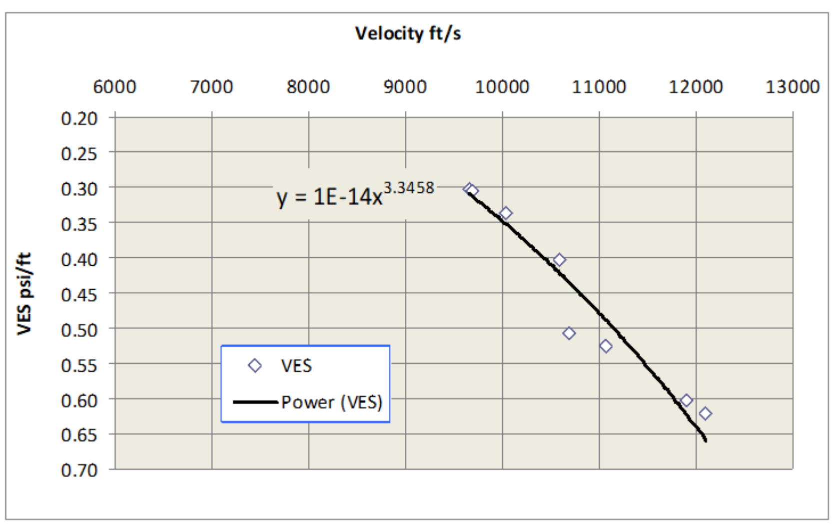

Fig. 10: A cross-plot of sonic velocity against vertical effective stress.

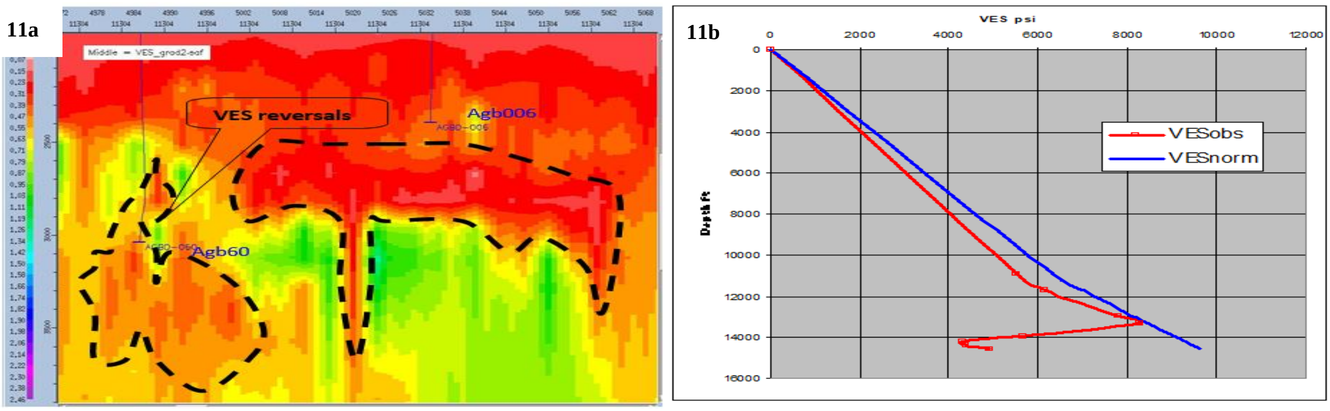

Fig. 11: (a) The final VES model for the study area. (b) VES versus depth plot from the well

The overburden pressure was derived from seismic velocity, according to Gardner's (1974) equation. For the study area of interest, the multiplying and power constants in Gardner's equation were taken as 0.068 and 0.382 respectively, consistent with the age of the sediments in the Agbada Basin (Okey et al.; 2021). Density data is cross-plotted with shale trend velocity, and a power curve is fitted into the data to derive a new density profile for the area. The new density is multiplied by a factor 0.433 to estimate overburden pressure gradient in psi/ft as shown in Fig. 12a. Overburden pressure is affected by the density of sediments and the vertical effective stress. A drop in VES and density occasioned by overpressures can be seen as a slight reversal on the overburden pressure plot (Fig. 13b).

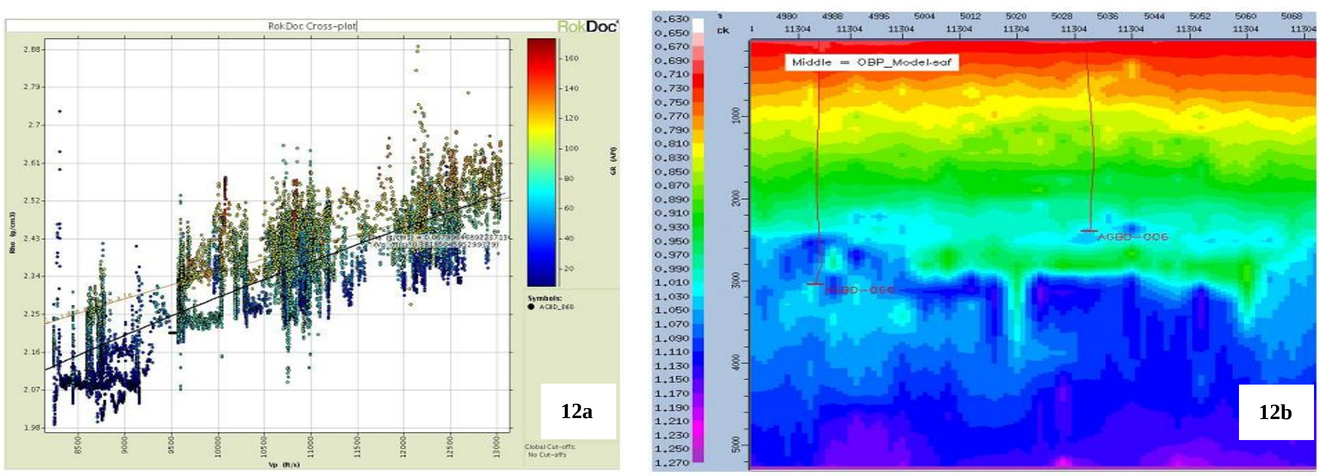

Fig. 12: (a) A cross-plot of density versus shale trend velocity. (b) The seismically overburden profile for the study area

Furthermore, the pore pressure was estimated from the Terzaghi (1943) relationship, subtracting the vertical effective stress from the overburden pressure. The pore pressure profile is shown in Fig. 13. The pressure trend agrees with the well, only within the depths where there are controls. The well log analysis actually started from approximately 10,000 ft (2500ms), to the base of the well (14,560 ft or 3650 ms). As seen in the seismic pore pressure profile, the overpressure was mild between 2500ms and 2650ms. Afterwards, hard overpressures set in from 2700ms to 3100ms, with values hitting 0.82 psi/ft as seen by the well. The VES profile as well as calibrated velocity profile for the vicinity area also reveal that well Agb006 has no overpressure issues. However, if drilling has to be done below 2350ms which is the depth of Agb006, there will be a lot of hard overpressure issues to contend with, as seen in the pore pressure profile and in the VES and seismic velocity profile. As a matter of fact between 2500ms to 3100ms, hard overpressures pervade an extensive area, away from the calibration well

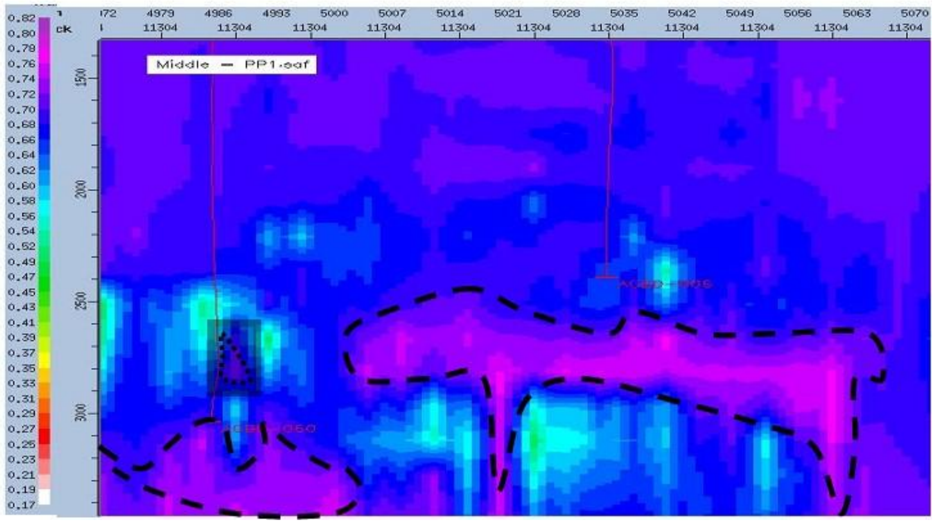

Fig. 13: 2D pore pressure profile for the study area.

The fracture gradient was estimated according to Hubert and Willis (1957) defined relative to pore pressure gradient, Poisson's ratio for wet shale and the vertical effective stress. The estimated fracture gradient is shown in Fig. 14, ranging in value from 0.68 to 0.86 psi/ft. The sudden jump in fracture gradient around 2500ms can be attributed to the onset of overpressures (Yassir & Bell, 1994). But at the vicinity well, the fracture gradient increases at a constant rate with depth because the pore pressure is hydrostatic (Zhang & Yin, 2017).

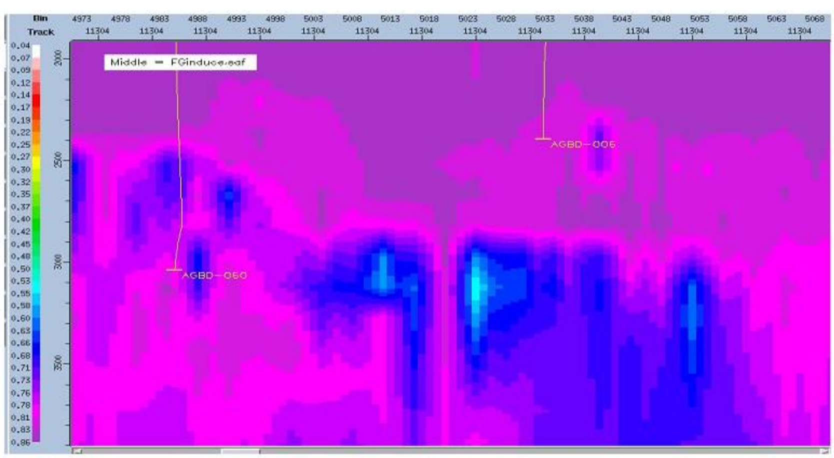

Fig. 14: The fracture gradient profile of the study area.

5. Conclusion

Pore pressures predicted from seismic velocities are most accurate when it can be shown that the seismic velocities are sensitive to changes in vertical effective stress as are sonic velocities measured from sonic logs within the area of interest. This research was therefore carried out to calibrate seismic velocities using well log data from a control well in the area of study with the intent of predicting pore pressures. The following conclusions were arrived at;

i. The predicted shale pressures from the calibration well show a normal hydrostatic trend from the surface down to about 10, 800 ftss, where a transition to overpressure was noticed.
ii. The pressure transition zone for this area, as estimated from the calibration log, can be said to be between 10,887ftss to 11702ftss, where mild overpressures ranging from about 0.51psi to 0.52psi were observed.
iii. The top of geopressure is found at approximately 13,318ftss, from where hard overpressures ranging from 0.77 to 0.79psi occurred in the shale and much higher in the reservoirs.

iv. Two regional marker shale (maximum flooding surfaces) control the over-pressures in the area; 19.4ma MFS (11707ftss) and 20.7ma MFS (13934ftss).

v. Vertical effective stress estimated from the seismic data showed reversalsaround the well and beyond, where overpressures occurred.

vi. The overburden pressure derived from seismic velocity showed that overburden pressure is affected by the density of sediments and the vertical effective stress,

vii. The seismic pore pressure profile showed the existence of mild to hard overpressures, with values as high as 0.82 psi/ft, within the vicinity of the calibration well.

viii. The estimated fracture gradient, defined relative to the pore pressure gradient, showed sudden jump in fracture gradient within the area of study, ranging in value from 0.68 psi/ft to 0.86 psi/ft.

References

Ateboh, P.E and Raimi, M. O. (2018). Corporate Civil Liability and Compensation Regime for Environmental Pollution in the Niger Delta. International Journal of Recent Advances in Multidisciplinary Research, 5(6), 3870-3873.

Abdali, M. R., Mohamadian, N., Ghorbani, H., & Wood, D. A. (2021). Petroleum well blowouts as a threat to drilling operation and wellbore sustainability: causes, prevention, safety and emergency response. Journal of Construction Materials: Special Issue on Sustainable Petroleum Engineering, 2652, 3752.

Bowers, G. L. (2001). Determining an appropriate pore-pressure estimation strategy. Paper presented at the Offshore technology conference.

Cathles, L. (2001). Capillary seals as a cause of pressure compartmentation in sedimentary basins. Paper presented at the Petroleum Systems of Deep-Water Basins: Global and Gulf of Mexico Experience. 21st Annual Bob F. Perkins Research Conference, Gulf Coast Section of the Society of Economic Paleontologists and Mineralogists [CD-ROM].

Chilingar, G. V., Serebryakov, V. A. and Robertson, J. O. J. (2002). Origin and Prediction of Abnormal Formation Pressures, Developments in Petroleum Science. Elsevier, Amsterdam, Netherlands.

Chopra, S., & Huffman, A. R. (2006). Velocity determination for pore-pressure prediction. The Leading Edge, 25(12), 1502-1515.

Corredor, F., Shaw, J. H., & Bilotti, F. (2005). Structural styles in the deep-water fold and thrust belts of the Niger Delta. AAPG bulletin, 89(6), 753-780.

Dutta, N. C. (1987). Fluid flow in low permeable porous media. Editions Technip, 567 - 595.

Eaton, B. A. (1972). Graphical method predicts pressure worldwide. World Oil, 182, 51 - 56.

Ejedawe, J. (1981). Patterns of incidence of oil reserves in Niger Delta Basin. AAPG bulletin, 65(9), 1574-1585.

Fertl, W.H., 1976. Abnormal Formation Pressures. Elsevier, Amsterdam, Netherlands.

Glireath, J. (1968). Electric log characteristics of diapiric shale. Memoir of the American Association of Petroleum Geologists, 8, 137-144.

Gunter, W. D., Bachu, S., & Benson, S. (2004). The role of hydrogeological and geochemical trapping in sedimentary basins for secure geological storage of carbon dioxide. Geological Society, London, Special Publications, 233(1), 129-145.

Ifeanyi, N. R. (2015). Comparing methods of predicting pore pressure. International Journal of Scientific & Engineering Research, 47(2), 77-90.

Johnson, H. A. and Bredeson, D. H. (1971). Structural Development of some Shallow Salt Domes in Louisiana Miocene Productive Belt. American Association of Petroleum Geologists Bulletins, 55 (2), 204 - 226.

Kumar, B., Niwas, S., & Mangaraj, B. K. (2012). Pore pressure prediction from well logs and seismic data. Paper presented at the 9th Biennial International Conference & Exposition on Petroleum Geophysics.

Magara, K. (1980). Comparison of Porosity-Depth Relation- Ships of Shale and Sandstone. Petroleum Geology, 3, 175 – 185.

Magbagbeola, O. A., Willis, B. J. (2007). Sequence stratigraphic and syndepositional deformation of the Agbada Formation Robertkiri field Niger Delta, Nigeria. American Association of Petroleum Geologists Bulletin, 91, 945 - 958.

Mouchet, J. P. and Mitchell, A. (1989). Abnormal pressures while drilling: Origins, predictions, detection evaluation: Paris, France, Editions Technip, 255 p.

Murray, G. E. (1961). Geology of the Atlantic and Gulf Coastal Province of North America. New York, Harper and Brothers.

Neuzil, C. E. (1995). Abnormal Pressures as Hydrodynamic Phenomena. American Journal of Science, 295, 742 – 786.

Nunn, J. A. (1996). Buoyancy-driven propagation of isolated fluid-filled fractures: Implications for fluid transport in Gulf of Mexico geopressured sediments. Journal of Geophysical Research: Solid Earth, 101(B2), 2963-2970.

Nwajide, C. S., & Reijers, T. J. A. (2001). Geology of the Southern Anambra basin: Sedimentary geology and Sequence Stratigraphy in Nigeria. 45-70, 133-197.

Okey, J. U., Davies O. A. and Baatee V. (2021), Pre-Drill Pore Pressure Prediction from Seismic Velocities: A Case Study of Agbada Field in Niger Delta, Nigeria, International Research Journal of Advanced Engineering and Science, 6 (3), 295-301.

Osborne, M. J., & Swarbrick, R. E. (1997). Mechanisms for generating overpressure in sedimentary basins: a reevaluation. AAPG bulletin, 81(6), 1023-1041.

Perry, E. A., and Hower, J. (1972). Late Stage Dehydration in Deeply Buried Pelitic Sediments. American Association of Petroleum Geologists. Bulletin, 56, 2013 – 2021.

Ruby, W. W. and Hubbert, M. K. (1959). Role of fluid pressure in mechanics of overthrust faulting, II. Overhrust belt in geosynclinals area of western Wyoming in light of fluid pressure hypothesis. Geological Society of American Bulletin, 70, 167-205.

Sayers, C.M. (2006). An introduction to velocity based pore pressure estimate. The leading Edge, 25 (12), 146 - 150.

Sayers, C. M., Woodward, M. J., & Bartman, R. C. (2002). Seismic pore-pressure prediction using reflection tomography and 4-C seismic data. The Leading Edge, 21(2), 188-192.

Schulz, W. H., McKenna, J. P., Kibler, J. D., & Biavati, G. (2009). Relations between hydrology and velocity of a continuously moving landslide—evidence of pore-pressure feedback regulating landslide motion? Landslides, 6(3), 181-190.

Swarbrick, R. E. (2002). Challenges of porosity-based pore pressure Prediction. CSEG Recorder, USA.

Swarbrick, R. E., Osborne, M. J. and Yardley, G. S. (2002). Comparison of overpressure magnitude resulting from the main generating mechanisms. American Association of Petroleum Geologists Memoir, 76, 1 - 12.

Terzaghi, K. (1943). The Theoretical Soil Mechanics. John Wiley and Sons Inc. New York, USA.

Tingay, M. R., Hillis, R. R., Swarbrick, R. E., Morley, C. K., & Damit, A. R. (2009). Origin of overpressure and pore-pressure prediction in the Baram province, Brunei. AAPG bulletin, 93(1), 51-74.

Traugott, M. (1997). Pore/fracture pressure determination in deep water. World Oil, 218, 68 – 70.

Udoh, N. B., Uko, E. D., Davies, O. A., & Udonam-Inyang, U. (2022). Detection of Overpressure using 3D Seismic Response in the AL Field in the Niger Delta, Nigeria. Quest Journals Journal of Research in Environmental and Earth Sciences, 8(6), 22-33.

Uko, E. D., Emudianughe, J. E., & Tamunobereton-ari, I. (2013). Overpressure prediction in the north-west niger delta, using porosity data. Journal of Applied Geology and Geophysics, 1(3), 42-50.

Ukpong, A. J., & Anyanwu, T. C. (2018). Late Eocene—Early Oligocene Foraminiferal Biostratigraphy and Paleoenvironment of Sediments from "Beta-24 Well" Niger Delta Basin, South Eastern Nigeria. South Eastern Nigeria, European Academic Research, 6(2), 871-891.

Yardley, G. S., and Swarbrick, R. E. (2000). Lateral Transfer: A Source of Additional Overpressure. Marine and Petroleum Geology, 17, 523 – 538.

Yassir, N., & Bell, J. (1994). Relationships between pore pressure, stresses, and present-day geodynamics in the Scotian Shelf, offshore eastern Canada. AAPG bulletin, 78(12), 1863-1880.

Zahid, K. M., & Uddin, A. (2005). Influence of overpressure on formation velocity evaluation of Neogene strata from the eastern Bengal Basin, Bangladesh. Journal of Asian Earth Sciences, 25(3), 419-429.

Zhang, J. (2011). Pore pressure prediction from well logs: Methods, modifications, and new approaches. Earth-Science Reviews, 108(1-2), 50-63.

Zhang, J., & Yin, S.-X. (2017). Fracture gradient prediction: an overview and an improved method. Petroleum Science, 14(4), 720-730.

Zhao, J., Li, J., & Xu, Z. (2018). Advances in the origin of overpressures in sedimentary basins. Petroleum Research, 3(1), 1-24.